XL CILAMCE
IBERO-LATIN AMERICAN CONGRESS ON COMPUTATIONAL METHODS IN ENGINEERING
NOVEMBER 11-14, 2019
Praiamar Natal Hotel & Convention Natal, RN-BRAZIL

NUMERICAL ANALYSIS OF THE HOLDING CAPACITY OF TORPEDO ANCHORS CONSIDERING SETUP EFFECTS

Guilherme K. Lopes
José R. M. de Sousa
Gilberto B. Ellwanger
kronemberger.guilherme@laceo.coppe.ufrj.br
jrenato@laceo.coppe.ufrj.br
gbe@laceo.coppe.ufrj.br
Department of Civil Engineering, Federal University of Rio de Janeiro
Av. Athos da Silveira Ramos, 149, 21941-909, Ilha do Fundão, Rio de Janeiro, Brazil

Abstract. Torpedo anchors have proven to be an outstanding alternative of fixed anchor point for taut leg mooring systems on Brazilian offshore fields. This type of anchor has low construction and fabrication costs, which are not dependent on water depth and withstands high vertical loads. Torpedo anchor has a "rocket" shape and its installation is given by free fall using heavy weights as the driving kinetic energy. Its driving process induces an excess pore water pressure generation and causes significant shearing and disturbance, which affects the stress, strain and strength characteristics of the soil surrounding the anchor. Immediately after installation, the holding capacity of the torpedo anchor is significantly reduced. Although, after the anchor is driven, holding capacity is observed to increase with time. This phenomenon is referred as setup. This paper presents a numerical based study of a finless torpedo anchor embedded in a purely cohesive isotropic soil using an axisymmetric nonlinear finite element model. The plasticity Cap model was chosen to describe the mechanical behavior of the soil. Anchor-soil interaction is simulated using surface-to-surface contact pairs with a penalty type contact property to represent friction behavior between the surfaces in contact. A number of analyses are conducted using Abaqus/CAE® in order to understand the response of this structure when considering setup effects. Additionally, a parametric study is also performed. The results indicated that soil permeability plays an important role into setup process. Furthermore, plasticity parameters are also investigated and the results followed a pattern of behavior on structure response.

Keywords: Torpedo anchors, Finite element method, Setup

1 Introduction

World's great demand for oil and gas has stimulated the development of new research focused on the design of offshore structures. Nowadays, due to the innovative nature of the equipment employed by offshore oil industry, the exploitation of oil and gas can be conducted for water depths over 3,000 meters. Sousa et al. [1] point out that to minimize the congestion of the sea bottom due to the high number of risers and mooring lines employed on floating production and drilling units in operation, taut-leg mooring systems are usually employed instead of catenary systems. Taut-leg mooring systems require fixed anchor points that are capable of sustaining high vertical horizontal and vertical forces. According to Ehlers et al. [2], some typical foundations employed by the offshore industry are suction anchors, vertical load anchors (VLAs) and suction embedded plate anchors (SEPLAs). However, the installation costs of these anchors surprisingly increases with water depth.

In this scenario, Wodehouse et al. [3] describe that the torpedo anchor has proven to be an outstanding alternative in Brazilian offshore fields. Additionally, according to Medeiros Jr. [4], this type of anchor has low construction and installation costs, which are not dependent on water depth and withstands high vertical loads. The torpedo anchor (Fig. 1) belongs to the group named dynamically installed anchors (DIAs). Besides the torpedo anchors, the existing DIAs also include OMNI-Max anchors and deep penetrating anchors (DPAs).

The torpedo anchor has a rocket shape with a varying number of flukes. Its installation is given by free fall from a designated height above the seabed using heavy weights as the driving kinetic energy. Its structure usually comprises four different components: a padeye that connects the first chain segment of the mooring line to the anchor; a ballasted shaft of carbon steel; a varying number of flukes, usually from 0 up to 4; and a conical tip that is designed to help the embedment of the anchor. The weight of typical torpedo anchors varies from 35 tons up to 98 tons (Sousa et al. [1]).

Figure 1. Typical torpedo anchor with four flukes: conical tip (left) and top view with detail of the padeye (right) (Sousa et al. [1]).

After a torpedo anchor is driven in saturated soil, it is observed that its pullout resistance often increases. This phenomenon is known as setup. Although the exact mechanism by which setup occurs is not completely understood (Houssain et al. [5], Komurka et al. [6], SIMULIA [7]), two process are believed to play an important role. The first, and the most significant of them, corresponds to an increase in the soil effective stresses associated with the dissipation of the excess pore pressure built up around the anchor during installation. The other one is associated with thixotropic bonding between the soil grains and some aging effects.

As soil consolidation progresses, the horizontal (or radial) effective stress increases in the soil at the interface between the soil and the anchor. This increase in the effective stress leads to a higher frictional resistance offered by the soil to the anchor. This results in an additional pullout resistance.

Some investigations about the setup process of driven DIAs have been carried out in the past few years. Hossain et al. [8] conducted many centrifuge tests for dynamically installed anchors and, with the

torpedo anchor geometry installed on calcareous silty soil. Approximately 80% of the long-term anchor capacity would be available within 1 year after anchor installation. Raie and Tassoulas [9] and Radgahar et al. [10] performed numerical analyses of the installation of finless torpedo anchors using a computational fluid mechanics (CFD) model and the subsequent setup phase. The authors observed that the time needed to achieve a consolidation ratio of 90% is considerably lower than the total time needed to achieve complete consolidation of the soil (100% of consolidation). Again, it was observed a significant increase of the holding capacity of the torpedo anchor analyzed after installation. Richardson et al. [11] conducted several experimental tests comparing the results obtained with some theoretical models, which indicated that 50% of the holding capacity of dynamically installed anchors are achieved over 35 to 350 days after installation. They also conducted that 90% of the operational holding capacity is achieved over 2.4 to 24 years after installation. The authors emphasize that these results are highly dependent on the soil properties where the anchor have been installed.

Considering the project and design of torpedo anchors, setup effects are not directly incorporated. Sousa et al. [1] mention that, in practice, a typical torpedo anchor is first loaded approximately 3 months after its installation. However, the imposed loads are much lower than its load capacity, as safety factors between 1.5 and 2.0 are employed into the anchor's design. Hence, there is still a gap of information with respect to the setup mechanism in torpedo anchor's design.

Therefore, in order to contribute for this task, a nonlinear axisymmetric finite element (FE) model is proposed here. A finless torpedo anchor embedded in a purely cohesive isotropic soil is analyzed. It is assumed that the anchor is "wished in place". Also, it was assumed that soil stress conditions immediately after the anchor installation can be obtained by means of Cavity Expansion Method (CEM). All analyses were carried out using Abaqus/CAE® [12]. In the following, the proposed FE model is described in detail before presenting the results of a parametric study obtained using this model.

2 Finite Element Modeling

2.1 Soil Modeling

The soil is modeled by a conventional approach that considers the porous medium as a multiphase material and it adopts the effective stress principle to describe its behavior. The medium is considered fully saturated and the wetting liquid is sea water.

Thus, the porous medium is modeled by attaching the finite element mesh to the solid phase and the fluid present inside the medium can flow through this mesh. As mentioned before, the mechanical part of the model is totally based on the effective stress principle. The effective stress principle was first mentioned by Terzaghi [13], and its fundamental equation can be written as:

$$\boldsymbol{\sigma}' = \boldsymbol{\sigma} - u, \tag{1}$$

where $\boldsymbol{\sigma}'$ is the effective normal stress, $\boldsymbol{\sigma}$ is the total normal stress and u is the pore pressure.

A continuity equation is, therefore, required for the fluid inside the voids of the soil, equating the rate of increase in the liquid mass stored at a point to the rate of mass of liquid flowing into the point within the time increment. This continuity statement is written in a variation form as a basis for finite element approximation, which is defined as:

$$\int_V \frac{1}{J}\frac{d}{dt}(J\rho_w n_w)dV = -\int_S \rho_w n_w \mathbf{n}\cdot\mathbf{v}_w dS, \tag{2}$$

where J is the ratio of the medium's volume in the current configuration to its volume in the reference configuration, ρ_w is the density of sea water, n_w is the volume ratio of free wetting liquid at a point, $\boldsymbol{n}$ is the outward normal to S and $\mathbf{v}_w$ is the average velocity of the wetting liquid relative to the solid phase (the seepage velocity). In this equation, V corresponds to the space occupied by a volume containing a fixed amount of solid matter, and S is the surface of interest of this space.

The sea water flow through the solid phase of the soil is described by Darcy's law. Darcy's law states that, under uniform conditions, the volumetric flow rate of the wetting liquid through a unit area of the medium, $sn\mathbf{v}_w$, is proportional to the negative of the gradient of the piezometric head, thus:

$$sn\mathbf{v}_w = -\hat{\mathbf{k}} \cdot \frac{\partial \phi}{\partial \mathbf{x}}, \tag{3}$$

where s is the saturation, n is the porosity of the porous medium, $\hat{\mathbf{k}}$ is the permeability of the medium and ϕ is the piezometric head, defined as:

$$\phi \overset{\text{def}}{=} z + \frac{u_w}{g\rho_w}, \tag{4}$$

where z is the elevation above some datum, u_w is the fluid pore pressure and g is the magnitude of the gravitacional acceleration, which acts in the direction opposite to z.

The linear material behavior of the soil is modeled as linear elastic. It uses the generalized Hooke's law and, in order to represent the nonlinear material behavior, the modified Drucker-Prager (DP) plasticity model, commonly referred as Cap model, was chosen. According to Helwany [14], plasticity Cap model is appropriate to represent soil behavior because it is capable of considering the effect of stress history, stress path, dilatancy, and the effect of the intermediate principal stress. The yield surface of this plasticity model consists of three parts: a DP shear failure (F_s), an elliptical cap (F_c), which intersects the mean effective stress axis at a right angle, and a smooth transition region between the shear failure and the cap (F_t), as shown in Fig. 2. These yield surfaces are expressed, respectively, as:

$$F_s = t - p.\tan\beta - d = 0, \tag{5}$$

$$F_c = \sqrt{(p - p_a)^2 + \left(\frac{Rt}{1+\alpha-\alpha/\cos\beta}\right)^2} - R(d + p_a\tan\beta) = 0, \tag{6}$$

$$F_t = \sqrt{(p - p_a)^2 + \left[t - \left(1 - \frac{\alpha}{\cos\beta}\right)(d + p_a\tan\beta)\right]^2} - \alpha(d + p_a\tan\beta) = 0. \tag{7}$$

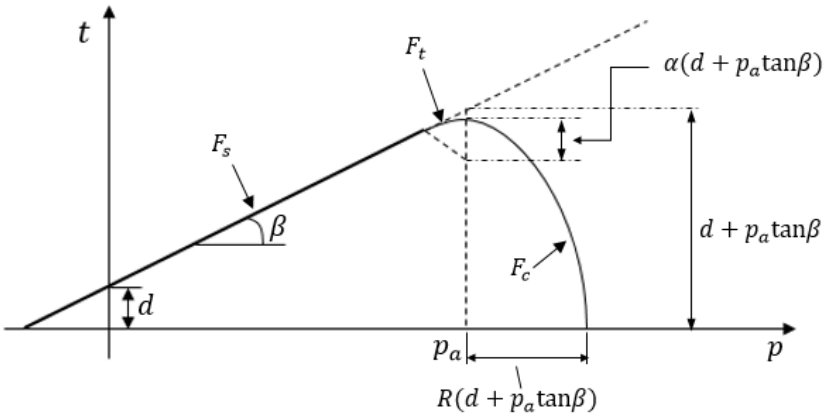

Figure 2. Yield surfaces of the Cap model in the *p*-*t* plane.

In this study, the hardening-softening behavior of the Cap model is simply described by a piecewise linear function relating the mean effective (yield) stress, p', and the volumetric plastic strain, ε_v^p. More details about this constitutive model are described by Helwany [14] and Dassault Systèmes [15].

2.2 Soil FE Mesh Characteristics

The undrained response of a torpedo anchor embedded in a clay is a classical elastoplastic problem that requires no volumetric locking and good bending behavior in order to obtain acceptable answers (Sousa et al. [1]). Moreover, as high plastic strains are expected in the soil, the elements may become highly distorted, and insensitivity to these distortions is demanded. Aiming at addressing these requirements, it was chosen, in Abaqus/CAE® [12], the use of continuous solid isoparametric axissymetric elements to represent the soil. Additionally, the elements used to represent the soil must account with an extra degree of freedom to save pore pressure values.

An overview of the main dimensions of the soil mesh is shown in Fig. 3. The proposed mesh is a

cylinder with a base diameter of $20D_a$. The height of the cylinder is given by the sum of the embedment depth of the anchor (H_p), the length of the anchor (L_a) and the distance of the tip of the torpedo to the bottom of the FE mesh (H_a).

The elements have dimensions varying between 0.10 m and 0.25 m in the regions where high plastic strains are expected to occur (close to the anchor) and between 0.25 m and 0.50 m in the regions far from the anchor, as shown in Fig. 3. The FE mesh was generated using the own interface of Abaqus/CAE® [12] and, as the proposed mesh is already very refined, it was assumed that the results obtained through the analyses are acceptable and with good precision.

Vertical and horizontal displacements of the soil cylinder are restrained at the nodes associated with its base. Displacements in the radial direction of the nodes associated with the outer wall of the cylinder are restrained but the displacements in the vertical direction are set free. This assumption allow that the self-weight of the soil can be applied on the first step of the analyses without any convergence problems.

Sousa et al. [1] performed several mesh tests in order to avoid any influence of the boundary conditions on the response of the anchor. They concluded that a diameter of $20D_a$ for the soil cylinder and a distance of 5 m for H_a dimension was enough to simulate an "infinite" media. Hence, these values were also considered in all analyses performed throughout this study.

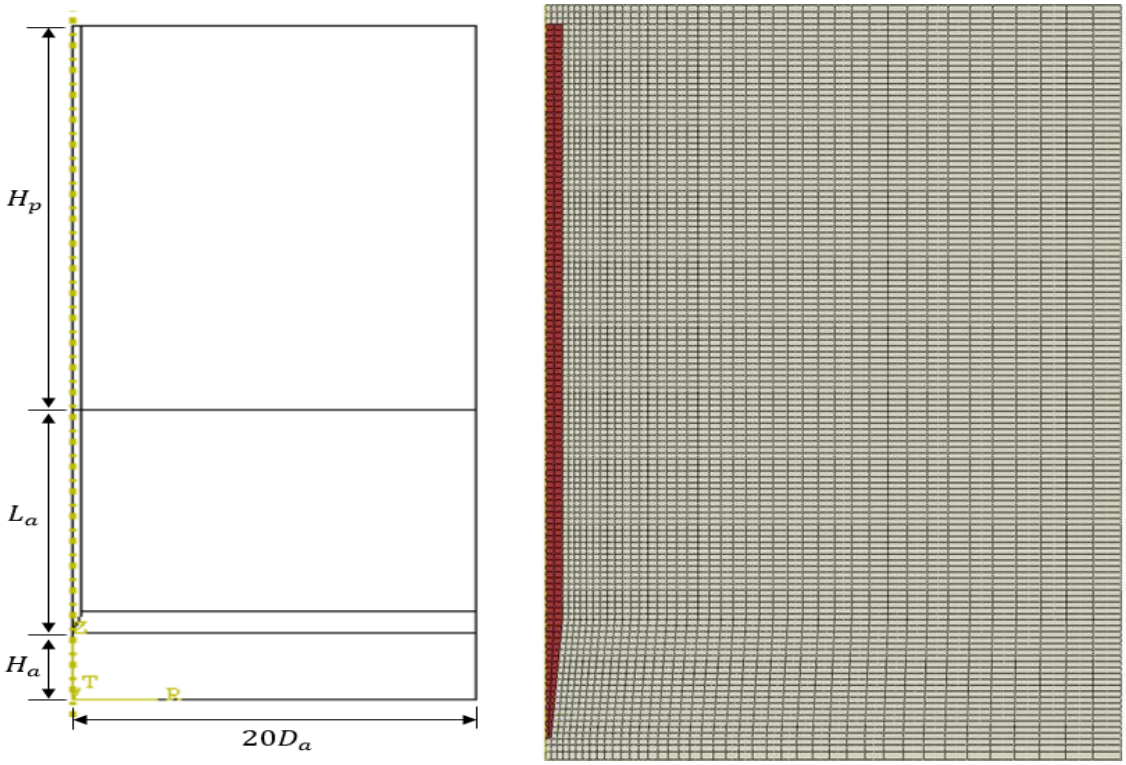

Figure 3. General view of the FE model.

2.3 Anchor modeling

The torpedo anchor is modeled with isoparametric solid elements analogous to the ones used to represent the soil but without the pore pressure degree of freedom. These elements, as shown before, are capable of considering both material and geometrical nonlinearities.

It is worth mentioning that neither the padeye at the top of the anchor nor the mooring line are represented in the proposed model. Hence, the load from the mooring line is applied at a node placed 1 m above the top of the anchor and it is rigidly connected to the top of the anchor by rigid bars using the beam MPC (Multiple Point Constraint) option in Abaqus/CAE® [12], as presented in Fig. 4.

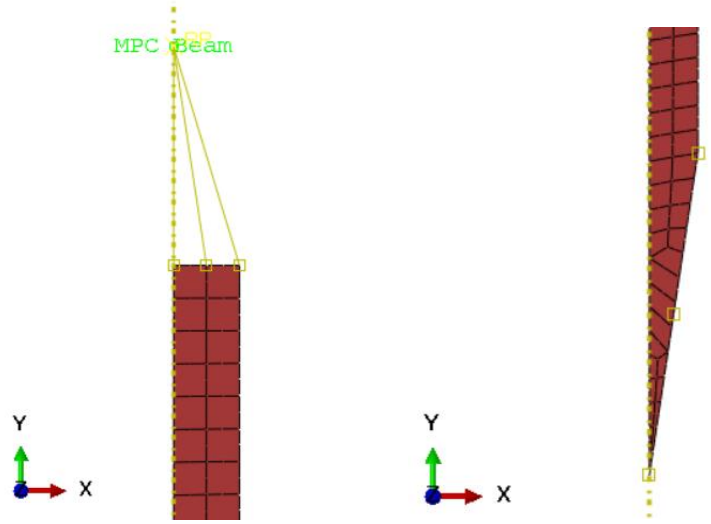

Figure 4. FE mesh details of the finless torpedo anchor: top view and load application (right) and bottom part of the tip (left).

Anchor loading is simulated through the application of a concentrated force on the reference node at a rate of 10.000 kN/s. This extremely high rate of loading is employed to ensure that the soil will behave in undrained conditions.

2.4 Anchor-soil interaction

Regarding problems involving contact between two boundaries, one of them is usually defined to be the master surface, and the other one as slave surface. These two surfaces together comprises the surface-to-surface contact pair. In surface-to-surface contact discretization type, each contact restraint is formulated based on an integral over a region around the corresponding node of the slave surface.

The slave surface is constrained against penetrating the master surface, and, usually, the master surface is defined to be the harder of the two. In the proposed model, as the anchor is much stiffer than the surrounding soil, all master elements are placed on the outer wall of the anchor and all slave elements are on the surrounding soil contact surface.

Another important aspect on the analysis refers to permeation between the materials, that is if there will be or not fluid flow between the soil and the anchor. As the pore pressure degree of freedom is only active on the soil elements, the FE program automatically considers the contact surface as impermeable; hence, no fluid flow will occur between the materials.

The interaction between the anchor and the soil is simulated using a penalty-type interface between them, which the main parameter is the friction coefficient between the surfaces in contact. According to Helwany [14], this kind of interface is capable of describing the frictional interaction between the structure surface and the surrounding soil in contact.

Karlsrud [16] states that pile axial loading capacity can be obtained calculating the shear resistance over the pile shaft with respect to time and effective radial stress. The author assumes that the effective radial stress over the pile can be multiplied by a factor, f_{cons}, varying between 0.2 and 0.4, according to the following equation:

$$f_{cons} \cdot \sigma'_r(U) = s_u(U), \tag{8}$$

where $\sigma'_r(U)$ is the effective radial stress with respect to soil degree of consolidation and s_u is the soil undrained shear strength.

However, during the analyses it was observed that when a factor equals to 0.2 was applied to the results corresponding to a radial effective stress at 100% consolidation, the values obtained were much higher than the ones of the soil with intact undrained shear strength. Thus, to bypass this problem, the factor was calibrated against the undrained shear strength corresponding to the soil fully reconsolidated.

In this case, it was assumed that the undrained shear strength of the fully reconsolidated soil is equal to the one recommended by the α-method from API [17]. Hence, the calibrated friction factor is given by:

$$f_{cons\_calib} = \frac{\alpha \cdot s_u}{\sigma'_{r(U=100\%)}}. \tag{9}$$

2.5 Initial stress state of the soil

Most geotechnical problems begin from a geostatic state, which is a steady-state equilibrium configuration of the undisturbed soil or rock under geostatic loading and it usually includes both horizontal and vertical components. In numerical modeling, it is important to establish these initial conditions correctly so that the problem begins from an initial equilibrium state.

An important aspect of the torpedo anchor analysis is the simulation of the initial stress state of the soil, i.e., the stresses in the soil prior to the application of any kind of structural load to the anchor. As the proposed FE model does not simulate the anchor penetration in the soil, stress changes in the soil surrounding the anchor are therefore claimed to be similar to those produced from the expansion of an ideal cylindrical cavity.

The Cavity Expansion Method (CEM) assumes that the strains induced from the anchor installation comes from ideal expansion of a cylindrical cavity. Randolph and Wroth [18] present a solution based on the assumption of a cylindrical cavity in an ideal elastic, perfectly plastic (EP) type soil model. They assume conditions of axial symmetry and plane strain, which imply that only radial displacement of soil particles will occur.

Hill [19] and Gibson and Anderson [20] demonstrate the expressions for the stresses around an expanded cavity. For a cavity expanded from zero radius to a radius r_0, the radial and circumferential stress changes within the plastic zone are given respectively by:

$$\Delta\sigma_r = s_u\left[1 + ln\left(\frac{G_{50}}{s_u}\right)\right] \tag{10}$$

$$\Delta\sigma_\theta = s_u\left[-1 + ln\left(\frac{G_{50}}{s_u}\right)\right] \tag{11}$$

The relationship between G_{50} and s_u can be estimated by the following empirical expression (Keaveny and Mitchell [21]):

$$\frac{G_{50}}{s_u} = \frac{e^{\left(\frac{137-\mathrm{IP}}{23}\right)}}{\left[1+\ln\left(1+\frac{(\mathrm{OCR}-1)^{3.2}}{26}\right)\right]^{0.8}} \tag{12}$$

where IP is the plasticity index of the soil and OCR is the overconsolidation ratio of the soil.

Further, Randolph and Wroth [15] estimate the excess pore pressure by assuming that the mean effective stress remains constant under undrained conditions. This initial distribution is such that the pore pressure is maximal at the anchor-soil interface and diminishes exponentially with radial distance from the center of the anchor. The distribution of the initial excess pore pressure can then be written as:

$$\Delta u_0 = \begin{cases} 2s_u(z)ln\left(\frac{r_p}{r}\right), & r_0 \le r \le r_p \\ 0, & r > r_p \end{cases}, \tag{13}$$

where $s_u(z)$ is the soil undrained shear strength varying with depth, r_p is the plasticized radius of the disturbed soil after anchor driving, and r_0 is the anchor radius.

In theory, the expansion of a cylindrical cavity is modeled with an initial radius of zero. In contrast, numerical calculations must begin with a finite cavity radius to avoid infinite circumferential strains. Carter et al. [22] found that doubling the cavity radius is adequate for both EP and modified Cam Clay models. Thus expanding a cavity from a_0 to $2a_0$ can approximate the cavity expansion from $r = 0$ to r_0, i. e. model the installation of an anchor with shaft radius of r_0. Though, for the analyses conducted in this study, it was considered a relationship of $a_0 = 0.5r_0$.

2.6 Solution procedure

A typical FE mesh to predict the load capacity of a finless torpedo anchor considering setup effects has approximately 100,000 degrees of freedom. As previously mentioned, the elements must account for contact, geometric and material nonlinearities.

Complete setup analysis is run, basically, in three consolidation steps. In the first one, the initial stress state of the soil (i. e. immediately after installation) is imported to the present model from a previous analysis where the CEM is simulated following the steps described by Lopes [23]. Briefly, the process consists on modeling the undisturbed soil with the in situ stress and, then, removing part of the soil and placing a rigid bar into it, creating a cylindrical cavity. Thus, the rigid bar is forced to move against the soil wall, as shown in Fig. 5, simulating the expansion of the cavity.

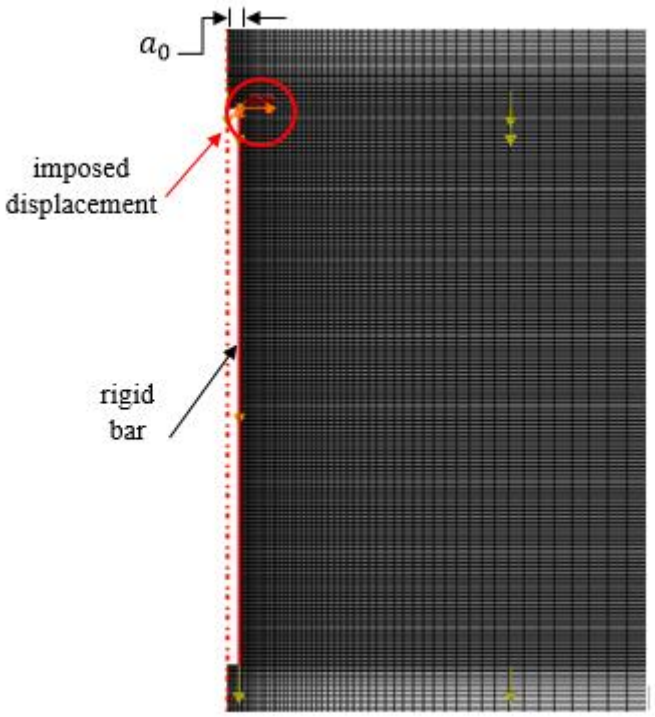

Figure 5. Detail of the rigid bar and its imposed displacement representing the simulation of the CEM (adapted from Lopes [23]).

The time for the first step is kept short in order to simulate the conditions of the soil immediately after anchor driving, so as not to allow the soil to consolidate. The second step involves continuing consolidation analysis for lengths of time varying from 10 seconds up to 100 million seconds (approximately 3.2 years). In this step, the excess pore pressure dissipates while the soil simultaneously consolidates as time progress. As the pore pressure dissipates, the radial effective stress in the soil adjoining the anchor also increases with time. This increase results in a higher frictional resistance between the soil and the anchor.

Finally, the third step involves the assessment of the pullout strength by applying a concentrated force at the reference node positioned above the top of the anchor and monitoring the vertical motion. As mentioned before, the load is applied at a high rate to ensure that the soil will behave in an undrained manner.

3 Parametric Study

3.1 Description

In this paper, various FE analyses were performed in order to study the importance of setup effects on the holding capacity of a finless torpedo anchor. Additionally, four parameters were varied in order to understand their influence on setup analysis. These parameters are the:

1. Coefficient of permeability of the soil (k);
2. Cap eccentricity parameter (R);
3. Cap transition surface parameter (α);
4. Cap flow stress ratio (K).

The soil is discretized using 8-noded axisymmetric elements with displacement and pore pressure degrees of freedom. It is considered to have an elastic modulus of 68.9 MPa, a Poisson ratio of 0.3 and a dry density of 1100 kg/m³. Cap model, with cohesion (d) of 0 kPa, friction angle (β) of 50.2°, cap eccentricity (R) of 0.4, transition surface radius (α) of 0.5, and flow stress ratio (K) of 1.0, is used for describing soil plasticity. The existence of a cap limits the amount of dilation when the soils gets deformed in shear. Permeability of the soil was set initially to 2.5e-10 m/s and an initial void ratio of 1.5 was considered in all analyses.

The finless torpedo anchor is considered to be elastic with an elastic modulus of 15 GPa and a Poisson ratio of 0.3. The anchor is discretized using 8-noded axisymmetric elements similar to the ones used for soil discretization, with displacement degrees of freedom only. This consideration implies that the interface between the anchor and the soil is automatically considered as impermeable and, thus, no pore fluid flow will occur across this interface. Main dimensions of the torpedo anchor analyzed are presented in Fig. 6 and, for all analyses, the submerged weight of the torpedo anchor was assumed to be equal to 650 kN.

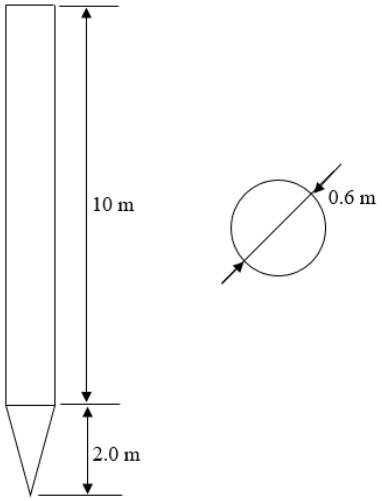

Figure 6. Main dimensions of the finless torpedo anchor.

It is worth mentioning that in this work, the anchor is supposed to be installed perfectly vertically, while, in practice, horizontal inclinations are often observed. In order to access only the effects of setup and plasticity of the soil on torpedo anchor's holding capacity, a unique embedment depth of 15 m was assumed in all analyses. It may not correspond to a real condition but it was kept to realize the parametric study.

3.2 Setup effects

The influence of setup effects on the holding capacity of torpedo anchors can be observed in Fig. 7. Results of the pullout resistance of the anchor are plotted for different instants of time after driving, varying from 10 seconds (simulating the scenario right after installation) and 10 years. Force vs. displacement curves are normalized with respect to anchor's weight, W_a, and anchor's external diameter (shaft diameter), D_a, respectively.

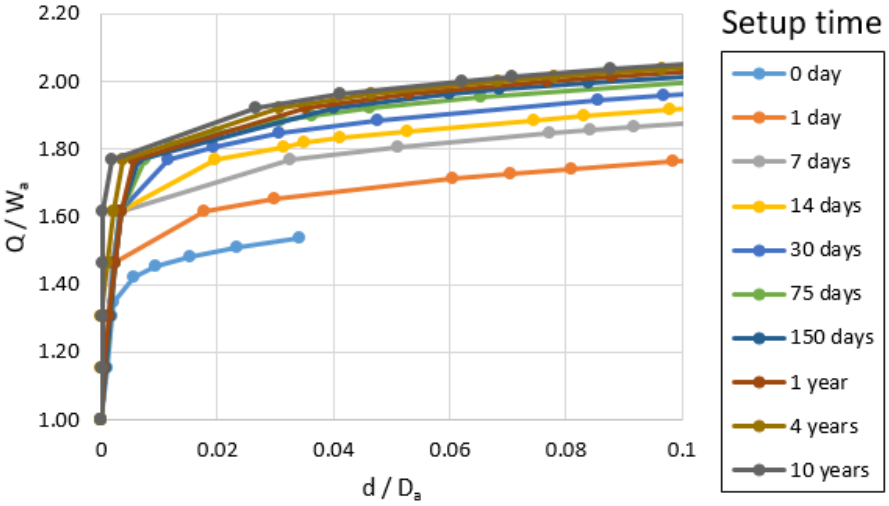

Figure 7. Torpedo anchor's normalized pullout capacity considering setup effects.

As expected, the anchor experiences an increase on its holding capacity whereas setup time advances. In general, the holding capacity of the finless torpedo anchor analyzed changes at a high rate for the first days after anchor installation, and this rate decreases as time progresses. Notice that the relationship between the holding capacity of the anchor, Q, and the anchor's weight is approximately 32% higher when comparing the results for setup times of 0 day and 10 years. It is emphasized that this behavior can also be observed for setup times greater than 150 days (5 months). This phenomenon can be better visualized when considering the setup curve shown in Fig. 8.

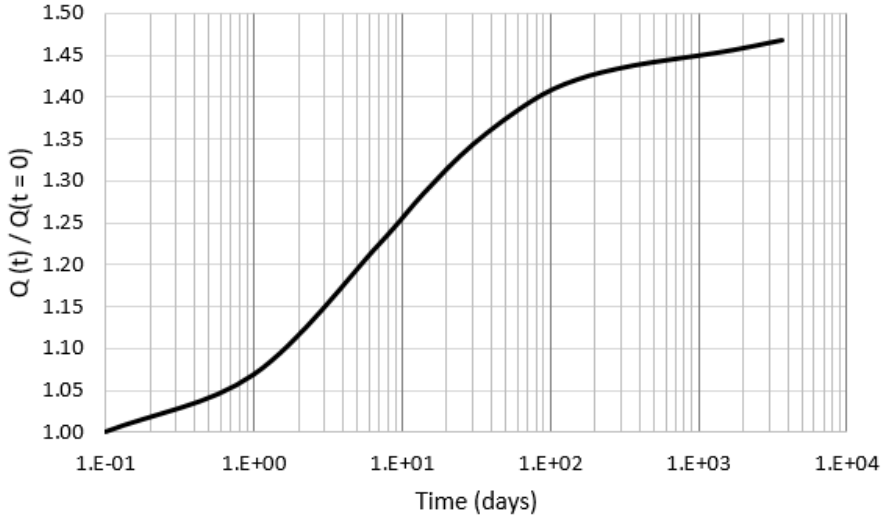

Figure 8. Torpedo anchor's setup curve.

Fig. 8 presents the setup curve for the torpedo anchor analyzed. The vertical axis shows the values of the normalized holding capacity of the anchor, which is the holding capacity at a time t after driving with respect to the holding capacity immediately after driving ($t = 0$). The three main phases of setup can be observed at Fig. 8. The first one, with a nonlinear rate of dissipation of excess pore pressure, comprised on the first day; the second phase, with a linear rate of dissipation of excess pore pressure with respect to the log of time, comprising consolidation times ranging from 1 to 150 days after driving; and the third phase, for consolidation times over 150 days.

The exact influence of the first phase of setup was not well reproduced by the numerical analyses and, hence, no further conclusions could be made with respect to this phase except for its approximate duration.

The results shown in Fig. 8 indicate that, for the present problem, the holding capacity of the torpedo anchor will be almost 50% higher after complete soil consolidation when comparing to the holding capacity at the end of driving. These results emphasize the importance of considering the setup effects on the project of torpedo anchors.

3.3 Permeability coefficient effects

As previously mentioned, it is stated that permeability coefficient dictates an important role at the reconsolidation of the remolded soil around the anchor. Fig. 9 shows soil consolidation ratio curves considering different permeability coefficients for an element of soil located on the soil-anchor interface corresponding to the midpoint of the anchor shaft (5 m below the top of the anchor). Soil consolidation ratio, U, is defined as:

$$U(t) = 1 - \frac{\Delta u(t)}{\Delta u(t=0)}, \tag{14}$$

where $\Delta u(t = 0)$ is the excess pore pressure immediately after anchor installation and $\Delta u(t)$ is the excess pore pressure at a time t.

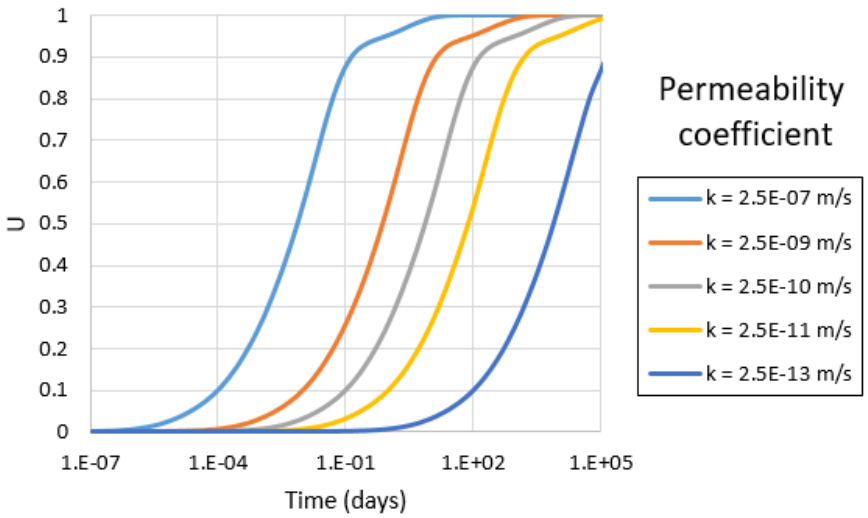

Figure 9. Consolidation ratio curves for different soil permeability coefficients.

Looking through the results presented in Fig. 9, it can be noticed that the time needed to achieve a higher consolidation ratio of the soil increases exponentially as time progresses. Furthermore, comparing the different soil consolidation curves, it can be observed that if the permeability coefficient of the soil is decreased by an order of magnitude then the soil consolidation ratio is proportionally increased. The same behavior can be observed when increasing or decreasing more than one order of magnitude of the permeability coefficient. It is important to notice that the values are not exactly the same as the ones multiplied by a factor of 10, but the expected results are very close to that.

3.4 Cap model parameters effects

In the present parametric study, three parameters of the Cap model were varied to understand their influence on the response of the anchor. These parameters are: flow stress ratio, K, transition surface parameter, α, and eccentricity parameter, R.

Effects of different values of K on anchor's holding capacity are presented in Fig. 10. According to Helwany [14], to ensure convexity of the yield surface, the range $0.778 \leq K \leq 1.0$ should not be violated. Values of K out of this range causes numerical problems and, consequently, analysis convergence is not achieved. From the graphic of Fig. 10, it can be concluded that the variation of the parameter K has low influence on the anchor response and it can be neglected. All curves follow the same format and distinguishes from each other just for a few units. It is emphasized that analysis convergence is achieved with fewer iterations when a value of $K = 1.0$ is used.

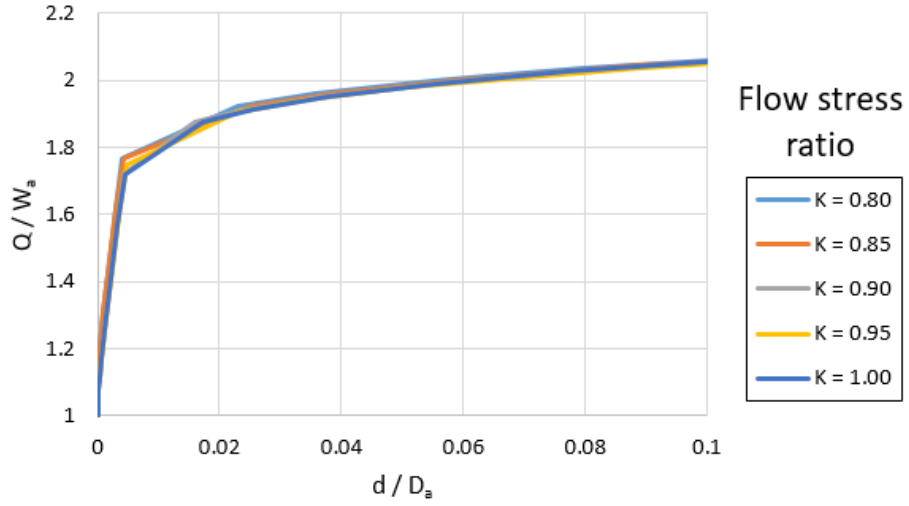

Figure 10. Influence of different flow stress ratios on pullout capacity.

The transition surface parameter, α, is generally a small number used to define a smooth transition surface between the Drucker-Prager shear failure surface and the cap surface. Fig. 11 shows the effects of different values of the transition surface parameter on anchor's holding capacity.

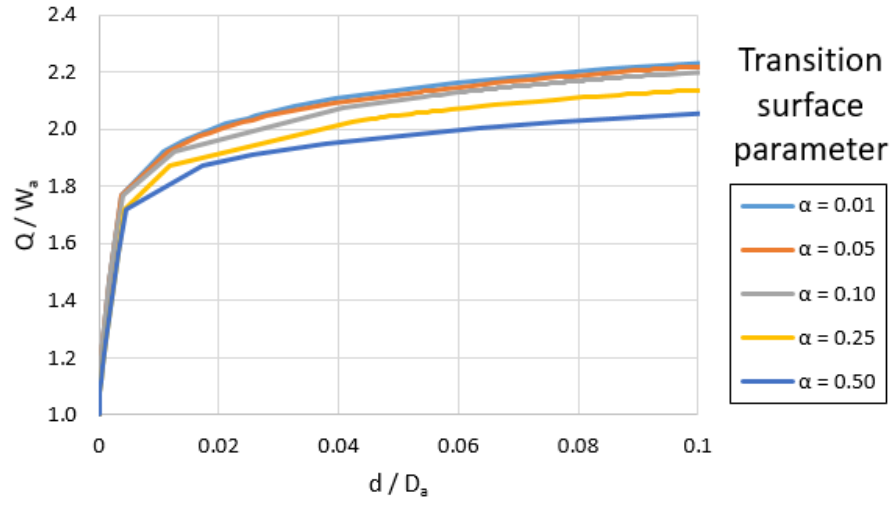

Figure 11. Influence of transition surface parameter on pullout capacity.

From the curves presented in Fig. 11, it can be observed that when values of the cap transition surface parameter ranging from 0.01 to 0.1 are employed, the estimated holding capacity of the anchor are practically the same. However, when higher values of this parameter are adopted, the response seems more conservative. In addition, it is important to emphasize that for small values (0.01 to 0.05) and higher values (0.5), numerical convergence is achieved with few iterations.

Finally, the eccentricity parameter of the Cap model was varied to investigate its influence on the holding capacity of the anchor. Fig. 12 present plots of the holding capacity of the torpedo anchor for different values of the eccentricity parameter. This parameter was varied downwards and upwards from the value used on the main analysis ($R = 0.4$).

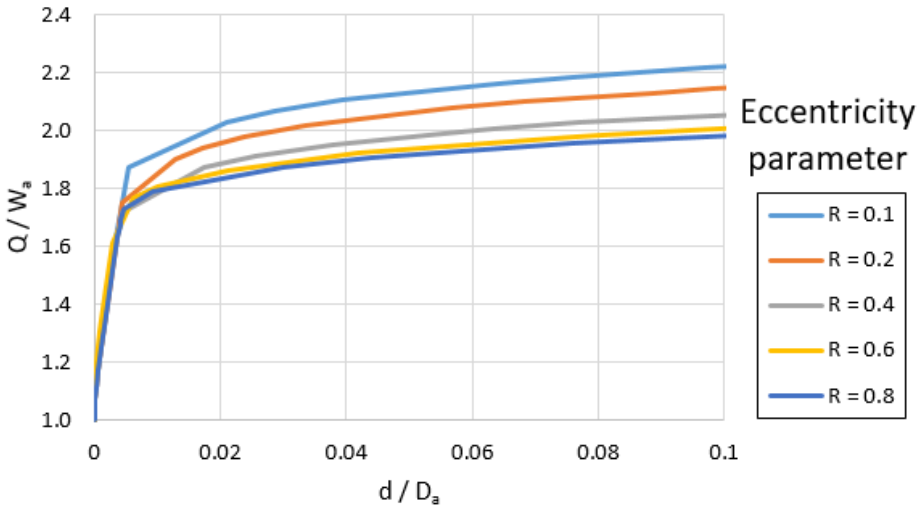

Figure 12. Influence of eccentricity parameter on pullout capacity.

It is notable the influence of this parameter on the determination of the anchor's holding capacity, through simple observation of the curves in Fig. 12. In general, as the value of the cap eccentricity parameter increases, the holding capacity estimated is more conservative. Furthermore, it seems to have a "lower limit" for the pullout capacity as the eccentricity increases, as the results obtained for $R = 0.6$ and $R = 0.8$ are closer.

Additionally, an analysis using the parameter $R = 0.01$ was performed but it did not converged until the end of the loading step. However, the pattern of the results seemed to the ones obtained on the analysis that used $R = 0.1$. On the other hand, analyses employing eccentricity parameter values over 0.8 do not achieve numerical convergence and no iteration on the loading step was concluded. Thus, this parameter appears to have a range of values that can be used and, the value of $R = 0.4$ used on the main analysis seems to be in good agreement to this range.

4 Conclusions

Numerical analyses conducted in this study contributed to confirm the importance of considering setup effects on the prediction of the holding capacity of torpedo anchors. Through the analyses it was stated that dissipation of the excess pore pressure represents the most significant mechanism associated with setup process, as it was expected. During soil reconsolidation, it could be observed a considerable increase on the effective stress at the anchor-soil interface and, consequently, an increase on shaft friction and on anchor holding capacity.

On the main analysis performed in this study, the finless torpedo anchor holding capacity was found to be approximately 32% higher than its initial value (immediately after installation), which is a considerable increase. Although the time needed for fully soil reconsolidation be over 10 years, a reasonable amount of recovery is noticed after 150 days after anchor installation. This implies that

approximately 5 months after anchor driving is somewhat found to be adequate on the design of this kind of structure and also being conservative.

The total time required to complete setup process depends largely on the coefficient of permeability of the soil, as could be observed in Fig. 9. Soils that have very low permeability, such as clayey soils, the complete setup time can be orders of magnitude larger than for soils with high permeability, which is the case of sandy soils. In addition, when approximately 80% of the setup is complete, the time range needed to get an increase on the anchor response is substantially larger than the time required at the beginning of the process.

Another important aspect observed about the influence of permeability coefficient is increasing its value in an order of magnitude (multiplying by a factor of 10), so that the time needed to achieve a specified consolidation ratio of the soil decreases in the same proportion. Thus, consolidation ratio of the soil will be an order of magnitude lower. The obtained value is not exactly as the one obtained by applying a factor of 10 but it is very close to that.

The plasticity constitutive behavior of the soil was also analyzed through this study. Some of the cap model parameters were varied in order to understand their influence on the structure's response. Flow stress ratio has almost no influence on the results as shown in Fig. 10. On the other hand, transition surface and eccentricity parameters appear to have a higher influence on predicting the holding capacity of the torpedo anchor. Nevertheless, the results obtained are in good agreement and this influence could be easily covered by the application of safety factors.

Acknowledgements

The study described in this paper is the result of a partnership between Petrobras and UFRJ. It was carried out with resources from the R&D program of the Electricity Sector regulated by ANEEL, under the PD-00553-0045/2016 project titled "Planta Piloto de Geração Eólica Offshore".

The authors would also like to express their gratitude to "Fundação Carlos Chagas Filho de Amparo à Pesquisa do Estado do Rio de Janeiro" (FAPERJ) and to "Coordenação de Aperfeiçoamento de Pessoal de Nível Superior" (CAPES), for the resources destined to the production of this research.

References

[1] J. R. M. de Sousa, C. S. Aguiar, G. B. Ellwanger, E. C. Porto and D. Foppa. Undrained load capacity of torpedo anchors embedded in cohesive soils. *Journal of Offshore Mechanics and Arctic Engineering*, 133 (2), 2011.

[2] C. J. Ehlers, A. G. Young and J. H. Chen. Technology assessment of deepwater anchors. *Proceedings of the 36th Offshore Technology Conference*, Houston, TX, 2004.

[3] J. Wodehouse, B. George and Y. Luo. The development of a FPSO for the deepwater Gulf of Mexico. *Proceedings of the 39th Offshore Technology Conference*, Houston, TX, 2007.

[4] C. J. Medeiros Jr. Low cost anchor system for flexible risers in deep waters. *Proceedings of the 34th Offshore Technology Conference*, Houston, TX, 2002.

[5] M. S. Houssain, Y. Kim and C. Gaudin. Experimental investigation of installation and pullout of dynamically penetrating anchors in clay and silt. *Journal of Geotech. and Geoenviron. Eng.*, 140(7), 2014.

[6] V. E. Komurka and A. B. Wagner. Estimating soil/pile set-up. Final Report, University of Wisconsin-Madinson, 2003.

[7] SIMULIA. Analysis of driven pile setup with Abaqus/Standard. Abaqus Technology Brief, 2007.

[8] M. S. Houssain, C. D. O'Loughlin and Y. Kim. Dynamic installation and monotonic pullout of a torpedo anchor in calcareous silt. *Géotechnique*, 65(2), pp. 77-90, 2015.

[9] M. S. Raie and J. L. Tassoulas. Simulation of torpedo anchor set-up. *Marine Structures*, 49, pp. 138-147, 2016.

[10] E. Radgahar, M. S. Raie and N. Motamani. Simulation of torpedo-shaped anchor (without fins) for submersible offshore platforms under tensile force. *Journal of Appl. Environ. Biol. Sci.*, 5(8S), pp. 107-111, 2015.
[11] M. D. Richardson, C. D. O'Loughlin, M. F. Randolph and C. Gaudin. Setup following installation of dynamic anchors in normally consolidated clay. *Journal of Geotech. Geoenvirom. Eng.*, 135(4), pp. 487-496, 2009.
[12] Dassault Systèmes. Abaqus/CAE 6.13-1. 2013.
[13] K. Terzaghi. The shearing resistance of saturated soils and the angle between the planes of shear. *Proceedings of the First International Conference on Soil Mechanics and Foundation Engineering*, vol. 1, pp. 54-56, 1936.
[14] S. Helwany. Applied soil mechanics with Abaqus applications. John Wiley & Sons, Inc., Hoboken, New Jersey, 2010.
[15] Dassault Systèmes. Abaqus 6.13 Online Documentation. Theory manual.
[16] K. Karlsrud. Prediction of load-displacement behavior and capacity of axially loaded piles in clay based on analyses and interpretation of pile load test results. Doctoral theses at NTNU, Trandheim, 2012.
[17] API. Recommended Practice for Planning, Designing and Constructing Fixed Offshore Platforms – Working Stress Design (RP 2A-WSD). American Petroleum Institute, 20th ed., USA, 2005.
[18] M. F. Randolph and C. Wroth. An analytical solution for the consolidation around a driven pile. *Intenational Journal of Numerical and Analytical Methods in Geomechanics*, vol. 3, pp. 217-229, 1979.
[19] R. Hill. The mathematical theory of plasticity. Oxford University Press, 1950.
[20] R. Gibson and W. Anderson. In situ measurement of soil properties with the pressumeter. Civil engineering and public works review, vol. 56, pp. 615-618, 1961.
[21] J. M. Keaveny and J. K. Mitchell. Strength of fine-grained soils using the piezocone. *Use of In Situ Tests in Geotechnical Engineering* (GSP 6), ASCE, Reston/VA, pp. 668-699, 1986.
[22] J. P. Carter, M. F. Randolph and C. Wroth. Stress and pore pressure changes in clay during and after the expansion of a cylindrical cavity. *International Journal for Numerical and Analytical Methods in Geomechanics*, vol. 3, pp. 305-322, 1979.
[23] G. K. Lopes. "Análise numérica da capacidade de cargas de âncoras torpedo considerando efeitos de setup". Master thesis, Federal University of Rio de Janeiro, RJ, Brazil, 2019.